

Theoretical and Experimental Inhibitive Properties of Mild Steel in HCl by ethanolic extract of *Boscia senegalensis*.

Femi Emmanuel Awe^{1*}, Suleiman O. Idris², Malik Abdulwahab³, Emeka E. Oguzie⁴.

¹ Department of Applied Chemistry, Federal University Dutsin-ma, Dutsin-ma, Nigeria.

² Department of Chemistry, Ahmadu Bello University, Zaria, Nigeria.

³ Department of Metallurgical and Material Engineering, Ahmadu Bello University, Zaria, Nigeria.

⁴ Electrochemical and Material Science Research Laboratory, Department of Chemistry, Federal University of Technology Owerri, Owerri, Nigeria.

*E-mail of the corresponding author: fawe@fudutsinma.edu.ng; Tel: (+2348065736306)

Abstract: The experimental aspect of the corrosion inhibition potentials of *Boscia senegalensis* was carried out using gravimetric and linear polarization techniques as well as scanning electron microscopy (SEM) and Fourier transform infrared spectroscopy (FTIR), whereas the theoretical aspect was done by using the Density functional theory (DFT) calculations to performed and model the electronic structures of some extract constituents, including Physiosorptive interactions with the Fe surface. The analyses of the experimental results showed that the inhibition efficiency increased with increase in concentration of the inhibitor and decreased with increase in temperature. The efficiency of the extract in HCl (70%). Thermodynamic parameters revealed that the adsorption of extract onto the metal surface was spontaneous, exothermic and supported the Physical adsorption process. FTIR results showed that the inhibition mechanism was by absorption process, through the functional groups present in the extract and that of the inhibited. Surface morphology also revealed that corrosion product confirmed the protection offered by the extract on the surface of the metal immersed in the acid media. The data obtained were fitted into various adsorption isotherms though the Freundlich isotherm was found to be best fit.

[Femi Emmanuel Awe, Suleiman O. Idris, Malik Abdulwahab, Emeka E. Oguzie. **Theoretical and Experimental Inhibitive Properties of Mild Steel in HCl by ethanolic extract of *Boscia senegalensis***. *Nat Sci* 2015;13(10):15-28]. (ISSN: 1545-0740). <http://www.sciencepub.net/nature>. 3

Keywords: Inhibition, density functional theory, corrosion, *boscia senegalensis*

1. Introduction

Industrial development is vital in the history of any developed country. Most industries use various types of metals including their alloy for the construction or fabrication of their plants and other installations. In most cases, contact between the metal and aggressive medium (such as acid, base and salt) is unavoidable (Eddy *et al.*, 2009 a, b). In view of the above, industrial facilities are exposed to corrosion and are often protected against corrosion by adopting several options including painting, oiling, cathodic and anodic protections, etc. However, the use of inhibitors has been found to be one of the best options available for the protection of metals against corrosion (Oguzie *et al.*, 2006; Abdallah, 2004 a, b). Numerous studies have been carried out on the corrosion of metals in different environments and their inhibition and most of the well-known inhibitors suitable for the inhibition of the corrosion of metals in acidic medium are heterocyclic compounds (Eddy *et al.*, 2010; Elayyoubi *et al.*, 2004; Ita, 2004 a, b; Ita and Offiong, 1997; Khavafar and Iran, 2006; Okafor *et al.*, 2007). For these compounds, their adsorption on the metal surface is the initial step of inhibition (Bilgic and Caliskan, 2001; El-Ashry *et al.*, 2006 a, b). The adsorption of inhibitor is linked to the presence of

heteroatoms such as N, O, P, and S and long carbon chain length as well as triple bond or aromatic ring in their molecular structure (Emregul *et al.*, 2003). Researches generally agreed that most of these plants are green inhibitors because they are biodegradable, less toxic and do not contain heavy metals (Okafor *et al.*, 2007). In the light of these, several plants extracts have been investigated and their corrosion inhibition properties are often attributed to its phytochemical constituent (Umoren and Ebenso, 2008). The exploration of natural products of plant origin as inexpensive and eco-friendly sources of important chemicals is an essential field of research; because more imaginative and targeted exploitation of the abundant phytochemical resources (alkaloids, tannins, flavonoids, amino acids, lignins, carbohydrates, etc.) could facilitate development of environmentally friendly alternatives to hazardous chemical processes. Plant extracts are used extensively in traditional medicine, where the phytochemical constituents have been shown to be effective against pathogenic (disease-causing) microorganisms and form the basis for several important pharmaceutical drug formulations (Okafor *et al.*, 2005; Raju and Maridas, 2011; Oyedeji *et al.*, 2005). Attempts to extend the field of application of these extracts to solving

materials corrosion problems in aqueous aggressive environments (chemical corrosion) and hence develop new, inexpensive, efficient and environmentally friendly corrosion-inhibiting additives from cheap and renewable sources are gaining increasing interest (Oguzie, 2008; Kumar, 2008; Ekanem *et al.*, 2010; Oguzie, 2005; Oguzie *et al.*, 2006; Satapathy *et al.*, 2009; Akalezi *et al.*, 2012; Oguzie *et al.*, 2012 a). Such studies are justified by the phytochemical constituents of the extracts, which have molecular and electronic structures bearing close similarities with those of conventional corrosion inhibitors and have been shown to also function through adsorption on the metal/corrosion interface. This report focuses on the application of plant extracts for metal corrosion control and investigates the inhibiting effect of extracts of *Boscia senegalensis* on the acid corrosion of mild steel.

2. Experimental

Materials used for the study were mild steel sheet of composition (wt %) Mn (0.6), P (0.36), C (0.15), and Si (0.03) and Fe (balance). The sheet was mechanically pressed cut into different coupons, each of dimension, 3cm x 2cm x 0.12 mm of thickness 0.12mm². Each coupon was polished with different size of emery paper grids (600 – 1200), and was later degreased by washing with ethanol, rinsed with acetone and air dried before they were preserved in a desiccator. All reagents used for the study were Analar grade and double distilled water was used for their preparation.

2.1 Plants Extraction

Samples of *Boscia senegalensis* leaves were obtained from Zango – Shanu, Sabon Gari Local Government, Kaduna State Nigeria. The samples were later taken to Herbarium in Department of Biological sciences, Ahmadu Bello University Zaria Nigeria for identification and was assigned a batch number. The leaves were dried, ground, and soaked in a solution of ethanol for 48 hours. After 48 hours, the samples were filtered. The filtrates were further subjected to evaporation at 352 K in order to make it free of ethanol. The stock solutions of the extract so obtained were used in preparing different concentrations of the extract by dissolving 0.1, 0.2, 0.3, 0.4, and 0.5 g of the extract in 1L of 1.0 M HCl, respectively. For gravimetric analysis as well as linear polarization analysis, the concentration of HCl used for the preparation of the inhibitor-acid solutions was 1.0 M.

2.2 Chemical analysis

Phytochemical analysis of the ethanol and aqueous extract of the sample was carried out according to the method reported elsewhere (Qureshi and Eswar, 2010). Frothing and Na₂CO₃ tests were used for the identification of saponin, bromine water,

ferric chloride tests were used for the identification of tannin while Leberman's and Salkowski's tests (Chloroform solution of the extracts with sulphuric acids and acetic acids) were used for the identification of cardiac glycosides while Dragendorf, Hager, and Meyer reagent tests (Potassium Mercuric Iodide and Solution of Potassium Bismuth Iodide) were used for the identification of alkaloid.

2.3 Scanning Electron Microscopy (SEM)

Morphological studies of the mild steel electrode surfaces exposed to uninhibited and inhibited 1.0 M HCl solutions for seven (7) days at 303K were taken by using a Jeol JSM – 7500F scanning electron microscope.

2.4 Gravimetric analysis

A previously weighed metal (mild steel) coupon was completely immersed in 250 ml of the test (in a close beaker). The beaker was inserted into a water bath maintained at a temperature of 303 K. After every 24 hours, each sample was withdrawn from the test solution, washed in a solution containing 50 % NaOH and 100 g/L of zinc dust. The washed steel coupon was rinsed in acetone and air dried before re-weighing. The difference in weight for a period of 168 hours was taken as the total weight-loss. The effect of temperature on mild steel corrosion and corrosion inhibition was investigated by performing experiments in 1.0 M HCl at 303, 313, 323 and 333 K for 3 hours immersion period. All tests were run in triplicates and the data showed good reproducibility. From the weight loss results, the inhibition efficiency (%I) of the inhibitor, the degree of surface coverage (θ), and the corrosion rate of mild steel (CR) were calculated using the equation 1, 2 and 3 respectively (Okafor *et al.*, 2010).

$$\begin{aligned} \% I &= (1 - W_1/W_2) \times 100 & 1 \\ \theta &= 1 - W_1/W_2 & 2 \\ CR \text{ (gh}^{-1}\text{cm}^{-2}\text{)} &= \Delta W/At & 3 \end{aligned}$$

where W_1 and W_2 are the weight losses (g/l) of mild steel in the presence and absence of inhibitor (in 1 M HCl) solution, respectively, θ is the degree of surface coverage, CR is the corrosion rate, ΔW - weight loss (grams), A - area of specimen (cm²), and t - period of immersion (hours).

2.5 Electrochemical measurements

Metal samples for electrochemical experiments were of dimensions 1.0 cm x 1.0 cm. These were subsequently sealed with epoxy resin in such a way that only one square surface of area 1.0 cm² was left uncovered. The exposed surface was degreased in acetone, rinsed with distilled water and dried in warm air. Linear polarization studies were carried out in the potential -1000 to 2000 mV at a scan rate of 0.333 mV

s⁻¹ at room temperature of 303K. Each test was run in triplicate to verify the reproducibility of the systems.

2.6 Fourier Transform Infrared Spectrophotometry (FTIR)

IR analyses of the inhibitor and that of the corrosion products (in the presence and absence of the inhibitors) was carried out using a SHIMADZU, FTIR-8400S Fourier Transform Infrared Spectrophotometer. The coupon was dipped in 250 mL of 1.0 M of HCl acid-inhibitor concentration for 7 days to form an adsorbed layer after which was retrieved, dried and scraped with a sharp razor blade. The scraps were collected for analysis. The samples were prepared using KBr and the analysis was done by scanning the sample through a wave number range of 400-4000 cm⁻¹ (Eddy *et al.*, 2008).

2.7 Theoretical modeling and simulation

All theoretical calculations were performed using the density functional theory (DFT) electronic structure programs Forcite and DMol³ as contained in the Materials Studio 7.0 software (Accelrys, Inc.).

3.0 Results and discussion

Preliminary phytochemical analysis Extracts of *Boscia senegalensis* reveal it contain a large number of phytochemical which include that saponnin, tannin, phlobatin, anthraquinone, cardiac glycosides, flavanoid, terpene, and alkaloid. The results of the phytochemicals are presented in Table 1; hence the inhibition efficiency of the ethanol extract of this plant may be due to the presence of these phytochemicals.

3.1 Inhibition studies

Figure 1 depicts the variation of weight loss of mild steel in uninhibited and inhibited 1 M HCl with exposure time. The plot reveals that the plant extract effectively retards the rate of corrosion of mild steel at all concentration. It is evident from the plot that weight losses of mild steel increases with increase in period of contact indicating that the rate of

corrosion of mild steel increases with increasing concentration of the acid. Table 2 presents the calculated inhibition efficiency and corrosion rate as a function of both immersion time and extract concentration. The results show that the additive was more effective at higher concentration. This means that the increase in corrosion rate of the mild steel specimen with immersion time did not significantly perturb the metal-inhibitor interactions and IE% maintains almost steady values. At higher temperature above the room temperature, the weight loss were found to be more higher than at room temperature and was also found to decrease with increase in concentration of inhibitors similar to those obtained at 303 K. However, the inhibition efficiency of ethanol extract of *Boscia senegalensis* decreases with increasing temperature. This also suggests that the adsorption of ethanol extract of *B. Senegalensis* on mild steel surface is consistent with the mechanism of physical adsorption. The evident stability of the corrosion inhibiting action of *B. senegalensis* extracts makes it rather attractive for actual practical applications.

Table 1: Phytochemical composition of the ethanol extract of *Boscia senegalensis*

		Phytochemicals	
Saponins		+	
Tanins		+	
Phlobatanins		+	
Anthraquinone		+	
Cardiac glycoside		+	
Flavanoid		+	
Terpene		+	
Alkaloid		+	

Note: + present

Table 2. Corrosion rates (CR) of mild steel and inhibition efficiencies (% I) of ethanol extract of *B.senegalensis*

Conc.(g/L)	10 ³ CR (gh ⁻¹ cm ⁻²)				I%			
	333K	323K	313K	303K	333K	323K	313K	303K
Blank	25.63	17.64	11.90	5.80	-	-	-	-
0.1	24.08	15.97	10.09	2.24	6.01	9.44	15.21	61.30
0.2	21.97	12.27	6.95	1.70	14.26	30.41	41.57	70.59
0.3	21.10	10.49	5.41	1.41	17.64	40.52	54.50	75.69
0.4	20.91	10.05	4.88	1.24	18.38	43.01	58.93	78.54
0.5	20.80	7.61	4.16	1.07	18.81	56.83	65.05	81.51

3.2 Linear polarization measurement

Polarization measurements are suitable for monitoring the progress and mechanisms of the anodic and cathodic partial reactions as well as identifying the effect of an additive on either partial reaction.

Linear polarization resistance experiments were thus carried out to understudy the effect of adsorbed plant extract on the kinetics of the anodic and cathodic processes. Figure 2 shows typical Linear polarization curves for the mild steel sample in 1-M HCl without

and with inhibitor. The electrochemical parameters derived from the polarization experiments are also presented in Table 3. The mild steel specimen is seen to exhibit active dissolution with no distinctive transition to passivation within the studied potential range in this environment. The plots also show that the anodic and cathodic reactions in blank acid follow

Tafel's law. It can be observed that both cathodic and anodic reactions were suppressed with the addition of various concentration of *Boscia senegalensis*, this implies that the plant extract functioned herein as a mixed-type inhibitor, reducing the rates of both anodic and cathodic reactions.

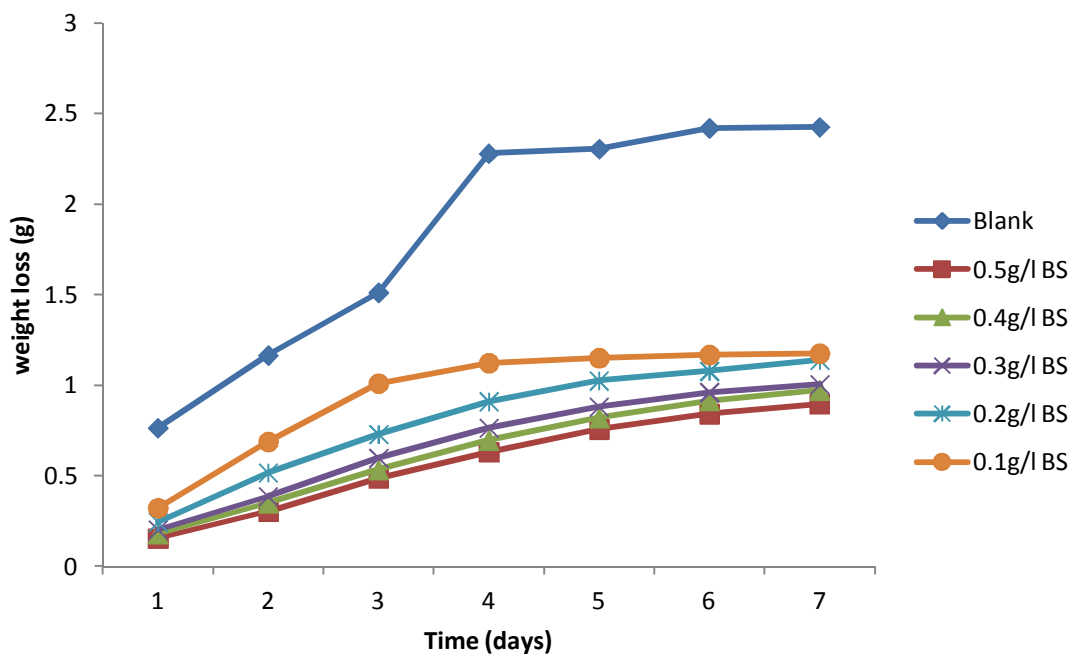


Fig. 1: Variation of weight loss with time for the corrosion of mild steel in HCl containing *Boscia senegalensis*

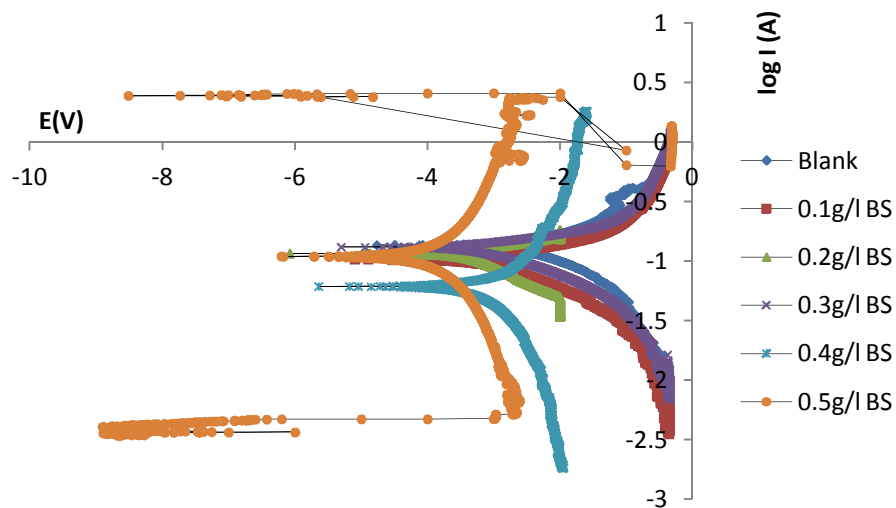


Fig. 2: Polarization curve for the corrosion of mild steel in 1.0 M HCl in the presence and absence of various concentration of *B. senegalensis*

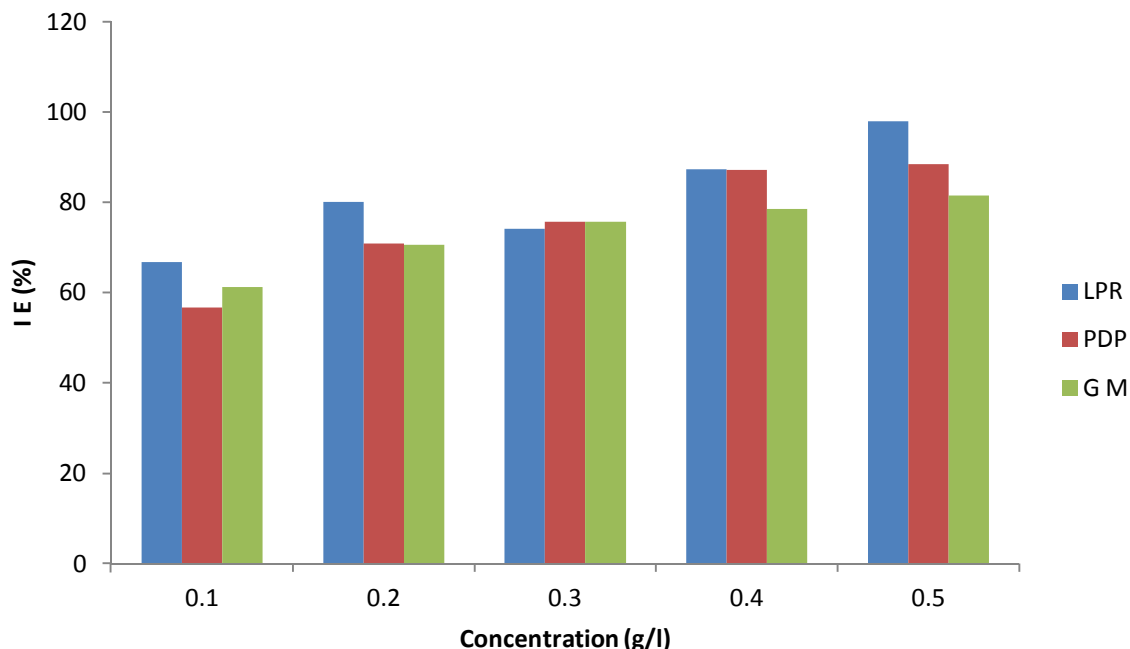


Fig. 3. Comparative chart of inhibitor efficiency (IE) for mild steel - 1 M HCl solution of *Boscia senegalensis*

Table 3: Polarization parameters for mild steel in 1.0 M HCl in the presence and absence of *B. senegalensis*

System	E_{corr} (mV vs SCE)	i_{corr} ($\mu\text{A}/\text{cm}^2$)	IE %
Blank	-864.95	1179.0	-
0.1	-986.68	511.00	56.65
0.2	-934.37	343.09	70.89
0.3	-882.40	286.53	75.69
0.4	-1212.4	151.07	87.18
0.5	-961.36	136.12	88.45

3.3

Adsorption Mechanism

Interaction between the corroding surfaces of the metal during corrosion inhibition can be explained in terms of its adsorption characteristics. In this study, results obtained for the degree of surface coverage at all temperature were fitted to a series of different adsorption isotherms. Fig. 4. Shows the freundlich adsorption isotherm for the plant extracts, from the result values of R^2 value were very high close to unity indicating a high degree of fitness adsorption data to the model. The tests revealed that Freundlich adsorption model best described the adsorption characteristics of the studied plant extract. It is also significant to note that the value of the adsorption equilibrium constant obtained from the intercept of

each adsorption isotherm is related to the free energy of adsorption according to the equation.

$$\Delta G_{\text{ads}}^{\circ} = -2.303RT \log (55.5K_{\text{ads}}) \quad 4$$

The standard Gibbs' free energy were calculated for the two adsorption isotherms at the various temperature for the plant extracts are also presented in Table 4, from the results obtained, the free energies are found to be negatively less than the threshold value of -40kJmol^{-1} , required for the mechanism of chemical adsorption to take place. Therefore, the adsorption of the studied plant extracts on both aluminium and mild steel surface is spontaneous and is consistent with the mechanism of physical adsorption (Lebrini *et al.*, 2010; Singh *et al.*, 2010; Loto, 2011).

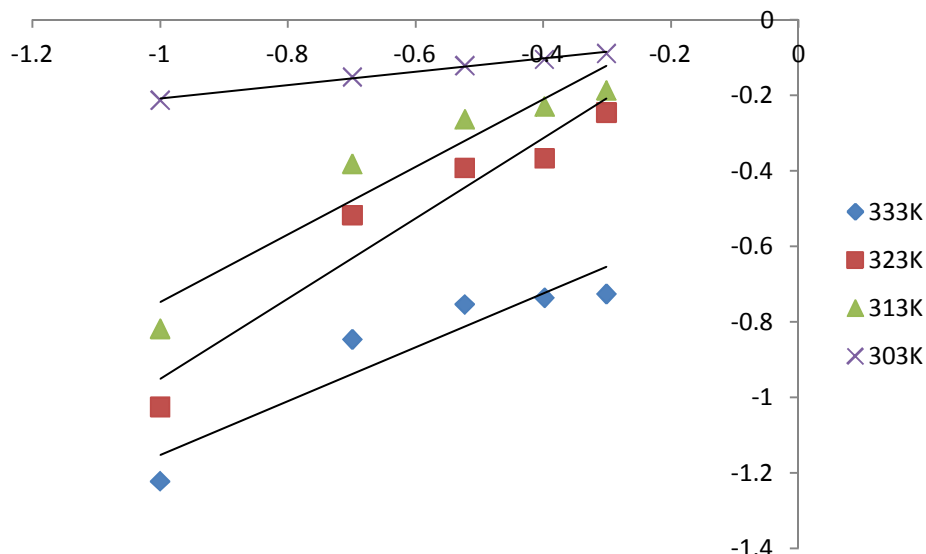


Fig. 4. Freundlich isotherm for the adsorption of BS on mild steel surface in 1.0 M HCl

Table 4: Adsorption parameters for the adsorption of ethanol extract of *B. senegalensis* on the surface of mild steel in HCl

	Temperature (K)	Slope	ΔG_{ads} (kJ/mol)	R^2
Isotherm	333	0.289	-8.31	0.537
	323	-0.062	-11.47	0.044
Langmuir	313	0.107	-11.32	0.136
	303	0.823	-9.93	0.999
Freundlich	333	0.71	-8.31	0.875
	323	1.062	-11.47	0.93
	313	0.892	-11.32	0.916
	303	0.176	-9.93	0.993

3.4

Effect of temperature

The adsorption of any organic inhibitor can affect the rate of corrosion either by decreasing the surface area or increasing the available surfaces for adsorption of the inhibitor on the surface of the metal. This is also considered by either affecting the activation energy of the anodic or cathodic reactions occurring in the inhibitor-free surface in the course of the inhibited corrosion process. The effect of temperature was studied with the transition state equation:

$$\log CR = \log A - E_a/2.303RT \quad 5$$

$$\log CR/T = \{ \log R/N_A h + \Delta S_a/2.303R \} - \Delta H_a/2.303RT \quad 6$$

where CR is the corrosion rate of the metal, A is the Arrhenius or pre-exponential factor, E_a is the activation energy (i.e the minimum energy needed before the corrosion reaction of the metal can

proceed), R is the universal gas constant and T is the temperature of the system.

Plot of $\log CR$ versus reciprocal of absolute temperature, $1/T$ from equation 5, as shown in Figure 5 gives a straight line with slope equal to $-E_a/R$, from which the activation energy for the corrosion process can be calculated.

Plot of $\log CR/T$ versus reciprocal of absolute temperature, $1/T$ from equation 6, as shown in Figure 6 gives a straight line with slope equal to $-\Delta H_a/2.303R$ and intercept of $\{ \log R/N_A h + \Delta S_a/2.303R \}$, from which the enthalpy and entropy of activation for the corrosion process can be calculated. Values of E_a , ΔS_a , and ΔH_a are presented in Table 3.

Values of the activation energy E_a extrapolated were found to be greater in inhibited than those obtained in blank suggesting the formation of an adsorption film of physical/electrostatic nature[28]. The heat of adsorption (Q_{ads}) of the ethanol extract was also calculated using the standard equation and found to be negative, which indicate that the

adsorption of the ethanol extract of *Boscia senegalensis* on the surface of the mild steel is exothermic. It is evident from Table 5 that the enthalpies of activation of the corrosion process to be positive which reflect endothermic nature of dissolution process.

The entropy of activation in the presence and absence of the inhibitor also has negative values which indicate that the activated complex in the rate determining step represents an association rather than dissociation, meaning that a decrease in disordering took place on going from the reactant to the activated complex (Lebrini *et al.*, 2011).

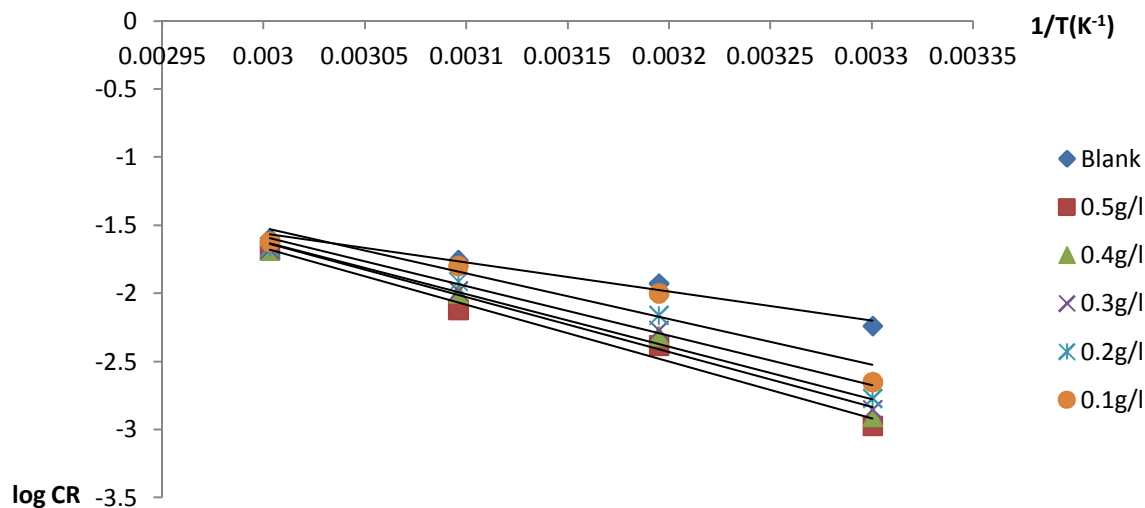


Figure 5. Plot of logCR against $1/T$ for mild steel in 1 M HCl solution in the absence and presence of various concentration of inhibitor

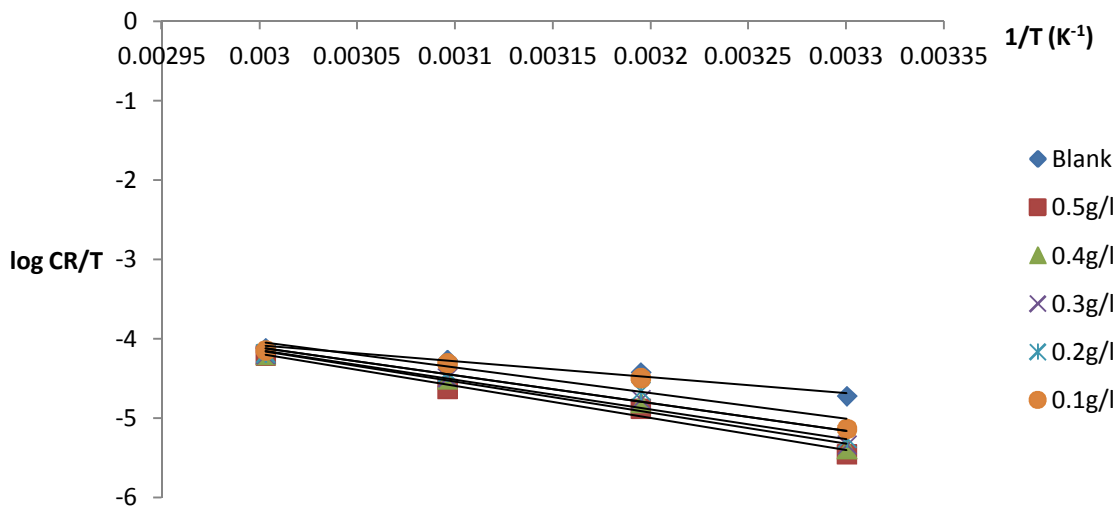


Figure 6. Plot of logCR/T against $1/T$ for mild steel in 1 M HCl solution in the absence and presence of various concentration of inhibitor

Table 5: Energy parameters for the dissolution of mild steel in HCl in the absence and presence of different concentration of *B. senegalensis*

Conc. (g/l)	E_a (kJ/mol)	ΔH_a (kJ/mol)	ΔS_a (kJ/molK ⁻¹)
Blank	41.55	38.22	-0.161
0.1	64.12	61.48	-0.091
0.2	69.48	66.84	-0.076
0.3	73.93	71.28	-0.063
0.4	77.35	74.73	-0.053
0.5	79.84	77.22	-0.046

3.5 SEM Analysis

Morphological studies of the surfaces of mild steel specimens in uninhibited and inhibited acid were followed by SEM after immersion in the test solutions for 7 days at 30 °C. Figures 7a and 7b present similar images for mild steel in uninhibited and inhibited 1 M HCl. A severely corroded surface morphology is

observed after immersion in the uninhibited systems, due to corrosive attack of the acid solutions Fig.7a. Corrosion was relatively general with no evidence of localized attack. With addition of BS extract Fig.7b, the corrosion damage is visibly reduced, and there is slight evidence of the adsorbate presence on the metal surface.

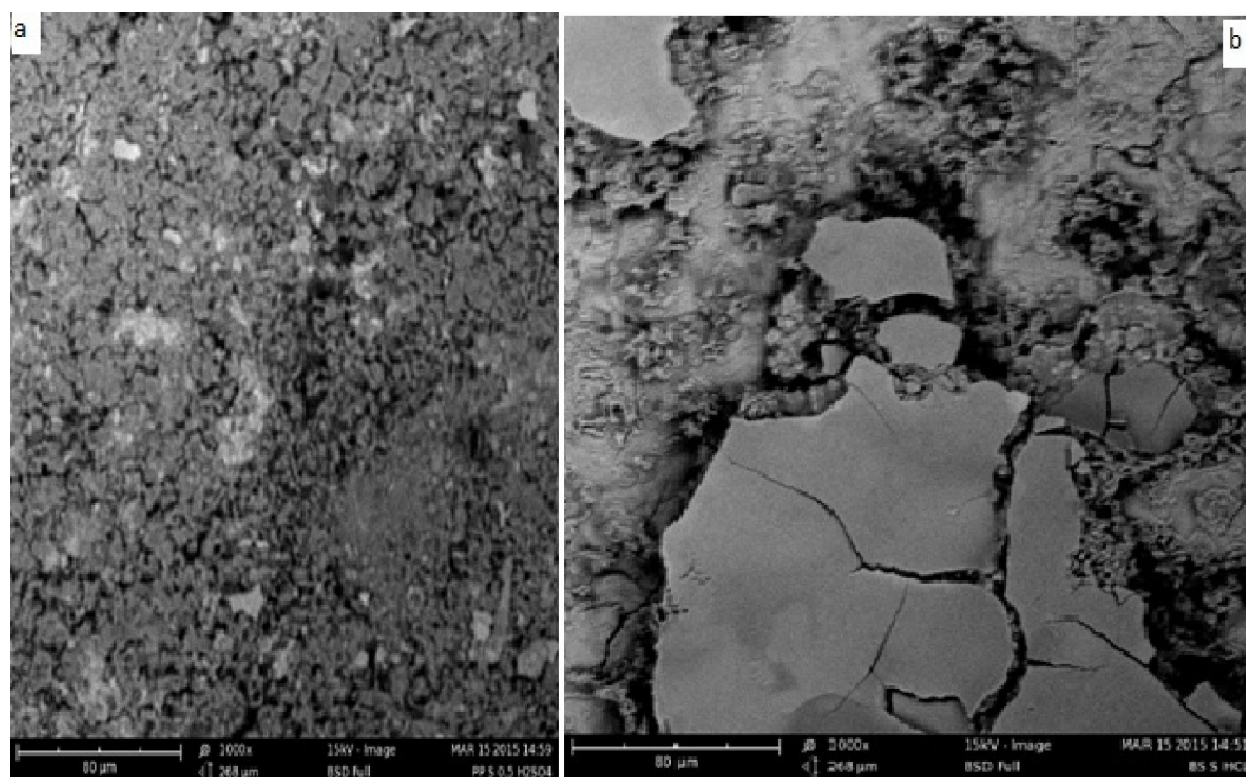


Fig.7. Micrographs of mild steel after dipping in 1.0 M HCl solution for 7 days at x 5,000 magnification (a). mild steel alone and in the presence of (b) BS

3.6

Infrared Spectroscopy analysis

The spectra of the powder as well as scrapped from the inhibitors films on the surface of the metal are presented in Fig. 8. From the results obtained, the aromatic stretch at 808cm⁻¹ was shifted to 800cm⁻¹, C-O stretch at 1065cm⁻¹ was shifted to 1180cm⁻¹, C-C stretch in ring at 1443cm⁻¹ was shifted to 1428cm⁻¹, N-H bend at 1628cm⁻¹ was shifted to 1624cm⁻¹ and O-H

stretch at 2931cm⁻¹ and 3423cm⁻¹ were shifted to 2527cm⁻¹ and 3405cm⁻¹. The shift in the frequencies indicates that there is interaction between the mild steel and the inhibitor (Okafor *et al.*, 2007). On the other hand, C-N stretch at 1265cm⁻¹ and C=O stretch at 1705cm⁻¹ were missing suggesting that these bond were used for adsorption of the inhibitor onto the surface of the mild steel.

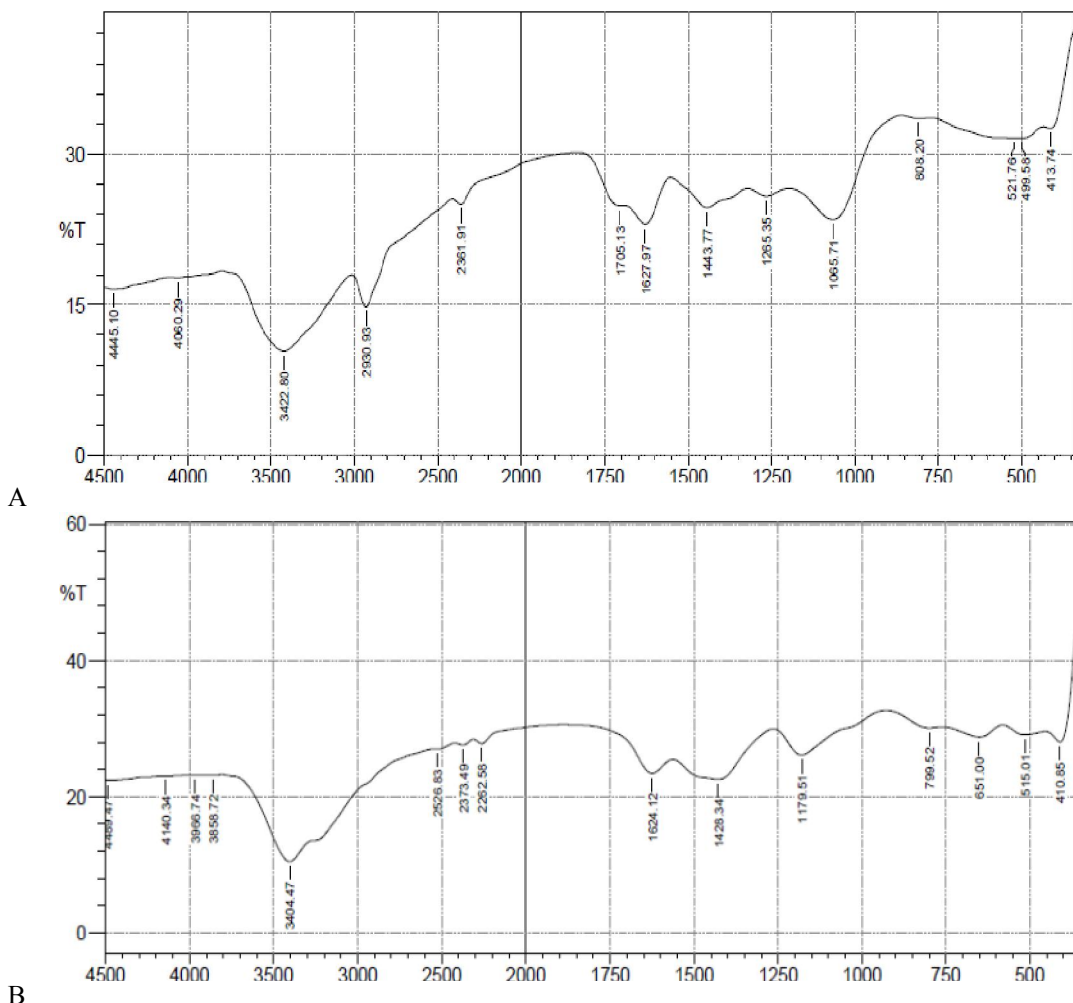


Fig. 8. FTIR spectra of (A) BS alone (B) corrosion product from the corrosion of mild steel when 0.5g/l of BS was used as an inhibitor in 1.0 M HCl

3.7 Theoretical modeling and simulation

The inhibiting action of BS extract is attributable to the adsorption of the phytochemical constituents (alkaloids, saponins, tannins, etc.) on the corroding mild steel surface. Precise experimental determination of the contributions of the different constituents to the overall inhibiting effect is considerably hindered by the complex chemical compositions of extracts. We thus relied on quantum chemical computations and molecular dynamics simulations to highlight the individual contributions of some extract constituents to the overall inhibiting effect. Calculations were performed to describe the electronic structures of some of the major chemical constituents of BS; 3-Chlorophenol, 3-Chloro-6-methylpyridazine, Hydroquinone and 3, 5-bis-(1,1-dimethylethyl)-phenol, with a view to establishing the active sites as well as local reactivity of the molecules. Simulations were performed by means of the density functional theory (DFT) electronic structure program DMol³

using a Mulliken population analysis (Delley, 1990; Delley, 2000). Electronic parameters for the simulation include unrestricted spin polarization using the DND basis set and the Perdew–Wang (PW) local correlation density functional.

Figure 9(a–d) illustrates the optimized structure, highest occupied molecular orbital (HOMO), lowest unoccupied molecular orbital (LUMO) of 3-Chlorophenol, 3-Chloro-6-methylpyridazine, Hydroquinone and 3, 5-bis-(1,1-dimethylethyl)-phenol respectively. The electron density is saturated all around each molecule; which should facilitate flat-lying adsorption orientations. The regions of high HOMO density are the sites at which electrophiles attack and represent the active centers, with the utmost ability to bond to the metal surface, whereas the LUMO orbital can accept the electrons in the d-orbital of the metal using antibonding orbitals to form feedback bonds (Martinez, 2003; Khaled, 2010b). The eigenvalues of the HOMO (E_{HOMO}) and LUMO

(E_{LUMO}) as well as the energy gap $\Delta E = E_{LUMO-HOMO}$ are presented in Table 6, together with some other quantum chemical parameters related to the molecular electronic structure of the most stable conformation of the molecules. High values of E_{HOMO} indicate the disposition of the molecule to donate electrons to an appropriate acceptor with vacant molecular orbitals, whereas low values of ΔE will favor good inhibition efficiencies because the energy to remove an electron from the last occupied orbital will be minimized (Rodríguez-Valdez *et al.*, 2005; Fu *et al.*, 2010; Fu *et al.*, 2011). The local reactivity of each molecule was analyzed by means of the Fukui indices (FI) to assess reactive regions in terms of nucleophilic and

electrophilic behavior. The f^- measures reactivity with respect to electrophilic attack or the propensity of the molecule to release electrons, whereas f^+ is a measure of reactivity relating to nucleophilic attack or tendency of the molecule attract electrons. The obtained values show that the molecules all have comparable E_{HOMO} values, which is not very surprising because the functional groups that comprise the HOMO are identical for all the molecules. The similarities in quantum chemical parameters mean that the adsorption strengths of the molecules would be mostly determined by molecular size parameters rather than electronic structure parameters.

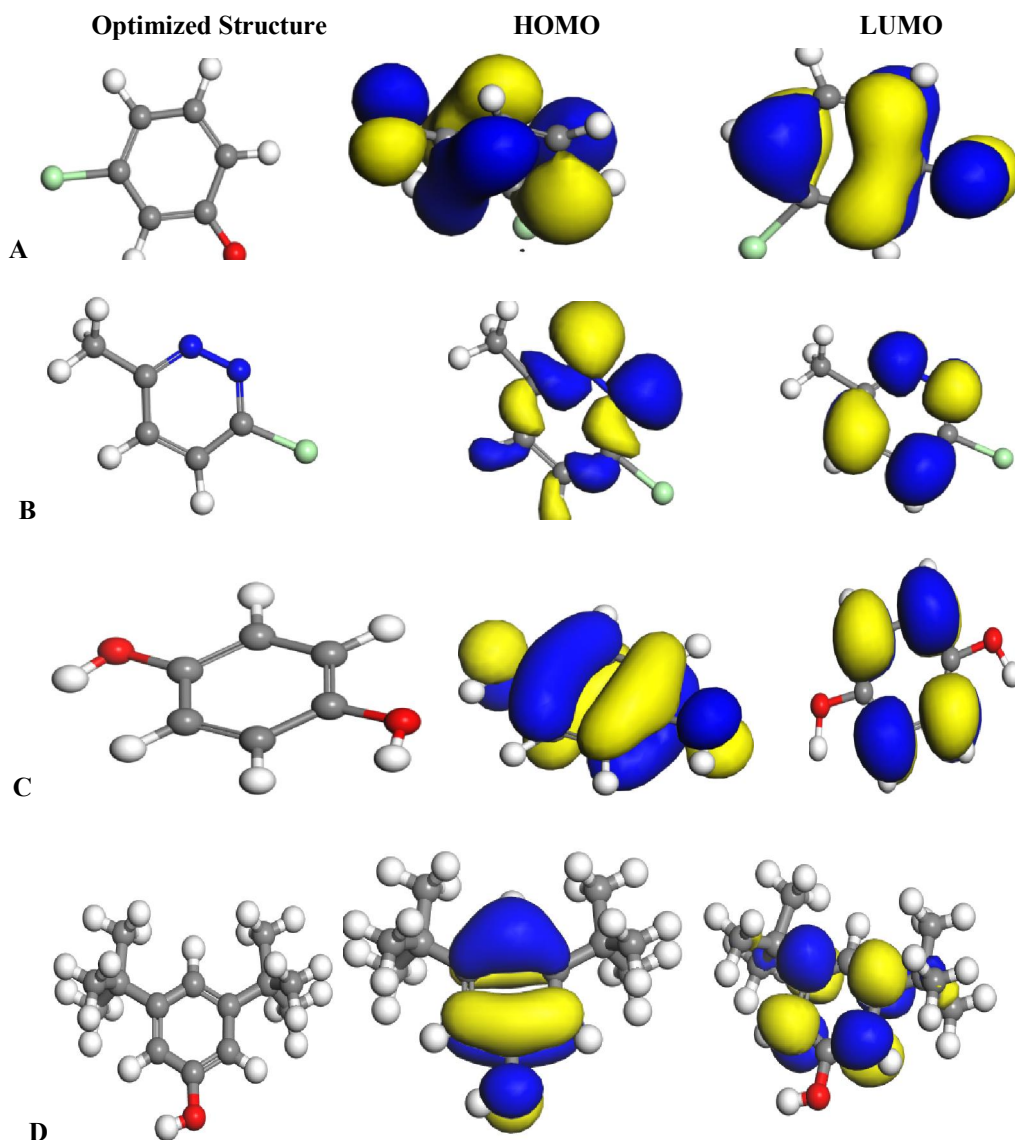


Fig. 9(a –d). Electronic properties of some constituents of *Boscia senegalensis* extract (atom legend: white = H; light gray = C; Red = O; blue = N). The blue and yellow isosurfaces depict the electron density difference, the blue regions show electron accumulation, while the yellow regions show the electron loss

Table 6. Calculated quantum chemical properties for the most stable configurations of some constituent of *Boscia senegalensis*

Property	3-Chlorophenol	3-Chloro-6-methylpyridazine	Hydroquinone	3, 5-bis(1,1-dimethylethyl)-phenol
$E_{HOMO}(eV)$	-0.2137	-0.1965	-0.1779	-0.1915
$E_{LUMO}(eV)$	-0.1177	-0.098	-0.0385	-0.0323
Max f- (Mulliken)	0.219 (O)	0.200 (N)	(O)0.118	0.135 (O)
Max f+ (Mulliken)	0.212 (O)	0.156 (Cl)	0.104(H)	0.096 (C)
Molecular weight(g/mol)	128	128	110	186
Adsorption energy (kcal/mol)	-63.25	-65.57	-57.79	-117.38

Adsorption of the different molecules on the metal surface was analyzed at a molecular level by molecular dynamics (MD) simulations, using Forcite quench molecular dynamics to sample many different low-energy configurations and identify the low-energy minima (Casewit et al., 1992 a, b). Calculations were carried out, using the COMPASS force field and the Smart algorithm, in a simulation box 30 Å X 25 Å X 29 Å with periodic boundary conditions to model a representative part of the interface, devoid of arbitrary boundary effects. The box composed of the Fe slab, cleaved along the (110) plane and a vacuum layer of 20 Å height. The geometry of the bottom layer of the slab was constrained to the bulk positions, whereas other degrees of freedom were relaxed before optimizing the Fe (110) surface, which was subsequently enlarged into a 10 X 9 supercell. The molecules were adsorbed on one side of the slab. Temperature was fixed at 350 K, with NVE (microcanonical) ensemble, with a time step of 1 fs and simulation time 5 ps. The system was quenched every 250 steps. Optimized structures of 3-Chlorophenol, 3-Chloro-6-methylpyridazine, Hydroquinone and 3, 5-bis-(1,1-dimethylethyl)-phenol and the Fe surface were used for the simulation.

Figure 10a–d shows representative snapshots of the top view (inset) of the lowest energy adsorption configurations for single molecules of 3-Chlorophenol, 3-Chloro-6-methylpyridazine, Hydroquinone and 3, 5-bis-(1,1-dimethylethyl)-phenol, respectively on the Fe (110) surface from the simulations. Each molecule can be seen to maintain a

flat-lying adsorption orientation on the Fe surface, as expected from the delocalization of the electron density all around the molecules. This orientation maximizes contact with the metal surface and hence augments the degree of surface coverage. The adsorption energy (E_{ads}) for the most stable configuration of the constituents on the Fe (110) surface was computed using the relationship below:

$$E_{ads} = E_{total} - (E_{mol} + E_{Fe})$$

E_{mol} , E_{Fe} and E_{total} correspond to the total energies of the molecule, Fe (110) slab and the adsorbed Mol/Fe (110) couple in the gas phase. A negative value of E_{ads} corresponds to a stable adsorption structure. The total energies were calculated by averaging the energies of the five most stable representative adsorption configurations. The obtained E_{ads} values; -63.25 kcal/mol for 3-Chlorophenol, -65.57 kcal/mol for 3-Chloro-6-methylpyridazine, -57.79 kcal/mol for Hydroquinone and -117.38 kcal/mol for 3, 5-bis-(1,1-dimethylethyl)-phenol are all negative and of considerable magnitude, suggesting stable adsorption structures. The trend in E_{ads} corresponds to the trend in molecular size, showing that the larger molecules are more strongly adsorbed on the metal surface. This strong affinity of the extract constituents for the Fe surface accounts for the remarkable corrosion inhibition efficacy of BS extract as observed experimentally.

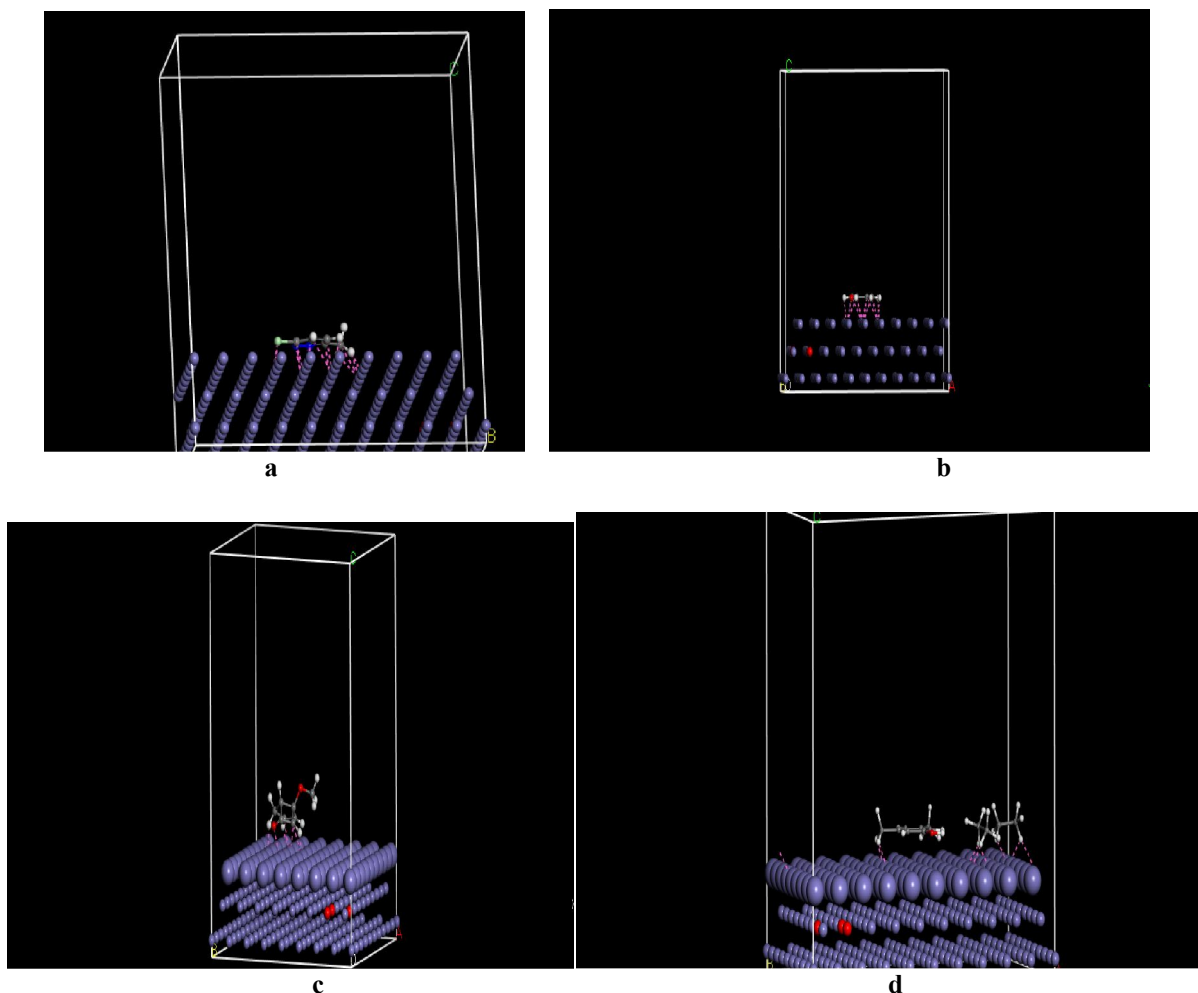


Fig. 10 Representative snapshots of a) 3-Chlorophenol b) 3-Chloro-6-methylpyridazine c) hydroquinone and d) 3, 5-bis-(1,1-dimethylethyl)-phenol on Fe (110) surface

Conclusions

This study has revealed that extracts of *Boscia senegalensis* effectively inhibit mild steel corrosion in 1 M HCl. Polarization measurements show that the inhibitor functioned via mixed-type mechanism, inhibiting the rates of both the anodic metal dissolution and cathode hydrogen ion reduction reactions. The results of SEM, and FTIR all indicate that the corrosion reaction was inhibited by adsorption of the extract organic matter on the corroding mild steel surface. The trends of inhibition efficiency with temperature as well as values of kinetic and activation parameters for corrosion and corrosion inhibition processes point toward significant Physisorption of the extract constituents on the mild steel surface. DFT-based quantum chemical computation was used to theoretically model the Physisorptive interactions between the plant extracts molecule, which is the active component of the extract, and Fe (110) surface. The magnitude of the obtained adsorption energy confirms strong Physisorption of the molecules.

Reference

1. Eddy, N. O., Odoemelam, S. A. and Ibiom (2009a). Adsorption and inhibitive properties of ethanol extract of *Costus afer* on the inhibition of the corrosion of mild steel in H₂SO₄. *J. Surface Sci. Technol.*, 25 (3-4):1-14.
2. Eddy, N. O., Ibok, U. J. and Ebenso, E. E. (2009b). Adsorption, synergistic inhibitive effect and quantum chemical studies on ampicillin and halides for the corrosion of mild Steel, *Journal of Applied Electrochemistry* DOI: 10.1007/s10800-009-0015-z.
3. Oguzie, E.E., Onuchukwu, A.I., Okafor, P.C. and Ebenso, E.E. (2006). Corrosion inhibition and adsorption behavior of *Occimum basicicum* extract on aluminum. *Pigment and Resin technology*, 35(2):63-70.
4. Abdallah, M. (2004a). Guar gum as corrosion inhibitor for carbon steel in sulphuric acid

- solutions. *Portugaliae Electrochimica Acta*, 22:161-175.
5. Abdallah, M. (2004b). Antibacterial drugs as corrosion inhibitors for aluminium in HCl solution. *Corrosion Science*, 46: 1981-1996.
 6. Eddy, N. O., Ebenso, E. E. and Ibok, U. J. (2010). Adsorption, synergistic inhibitive effect and quantum chemical studies of ampicillin (AMP) and halides for the corrosion of mild steel in H₂SO₄. *Journal of Applied Electrochemistry*, 40: 445-456.
 7. Elayyoubi, S.B., Hammouti, S., Kertit, H.O. and Maarouf, E.B. (2004). Corrosion inhibition of mild steel in hydrochloric acid solutions by malonitrile compounds. *Rev. Met. Paris*, 2:153-157.
 8. Ita, B.I. (2004a). 4-Formylmorpholine hydrazone and 4-formymorpholine: New corrosion inhibitors for mild steel in 0.1M hydrochloric acid solution. *Proccurement Of the Chemical Society Of Nigeria* (Suppl. to the J. of the Chem).
 9. Ita, B.I. (2004b). A study of corrosion inhibition of mild steel in 0.1M hydrochloric acid by O-vanilin hydrazone. *Bulletine of Electrochemistry*, 20(8):363-370.
 10. Ita, I.B. and Offiong, O.E. (1997). The inhibition of mild steel corrosion in hydrochloric acid by 2,21-pyridil and _pyridon. *Materials Chemistry and Physics*, 51:203-210.
 11. Khavasfar, A. and Iran, M. (2006). Study of organic corrosion inhibition on CO₂ corrosion of mild steel by electrochemical measurements. Paper presented at the 5th Internal surface engineering congress. Seattle, Washington. May 16, 2006.
 12. Okafor, P.C., Osabor, V. and Ebenso, E.E. (2007). Eco friendly corrosion inhibitors: Inhibitive action of ethanol extracts of *Garcinia Kola* for the corrosion of aluminium in acidic medium. *Pigment and Resin Technology*, 36(5):299-305.
 13. Bilgic, L. and Caliskan, N. (2001). An investigation of some Schiff bases as corrosion inhibitors for austenite chromium-nikel steel in H₂SO₄. *Journal of Applied Electrochemistry* 31:79-83.
 14. El Ashry, E.H., El Nemr, A., Essawy, S.A. and Ragab, S. (2006b). Corrosion inhibitors part III: quantum chemical studies on the efficiencies of some aromatic hydrazides and Schiff bases as corrosion inhibitors of steel in acidic medium. *ARKIVOC* 11:205–220.
 15. El Ashry, E.H., El Nemr, A., Essawy, S.A. and Ragab, S. (2006a). Corrosion inhibitors Part II: quantum chemical studies on the corrosion inhibitions of steel in acidic medium by some triazole, oxadiazole and thiadiazole derivatives. *Electrochimica Acta*, 51:3957–3968.
 16. Emregul, K.C., Kurtaran, R. and Atakol, O. (2003). An investigation of chloridesubstituted Schiff bases as corrosion inhibitors for steel. *Journal of Corrosion Science* 45:2803-2817.
 17. Umoren, S.A. and Ebenso, E.E. (2008). Studies of anti-corrosive effect of *Raphia hockeri* exudates gum-halide mixtures for aluminium corrosion in acidic medium. *Pigment and Resin Technology* 37(3):173-182.
 18. Okafor, P.C., Ekpe, U.J., Ebenso, E.E., Umoren, E. S. and Leizou, K.E. (2005). Inhibition of mild steel corrosion in acidic medium of sativum. *Bulletin of Electrochemistry*, 21(8):347-352.
 19. Raju, G., and Maridass, M. (2011). *Nat Pharm Technol* 1:19.
 20. Oyedeji, O. A., Adeniyi, B. A., Ajayi, O., and Ko'nig, W. A. (2005). *Phytother Res* 19:362.
 21. Oguzie, E. E. (2008). Corrosion Inhibitive Effect and Adsorption Behaviour of *Hibiscus Sabdariffa* Extract on Mild Steel in Acidic Media. *Portugaliae Electrochimica Acta* 26: 303-314.
 22. Kumar, A. (2008). Corrosion inhibition of mild steel in hydrochloric acid by sodium laury sulphate. *Electronic Journal of Chemistry*, 5(2): 275-280.
 23. Ekanem, U. F., Umoren, S. A., Udousoro, I. I., and Udoh, A. P. (2010). *J Mater Sci* 45:5558. doi:10.1007/s10853-010-4617-y.
 24. Oguzie, E.E. (2005). Inhibition of acid corrosion of mild steel by *Telfaria occidentalis* extract. *Pigment and Resin Technology*, 34(6): 321-326.
 25. Oguzie, E.E., Onuchukwu, A.I., Okafor, P.C. and Ebenso, E.E. (2006). Corrosion inhibition and adsorption behavior of *Occimum basicicum* extract on aluminum. *Pigment and Resin technology*, 35(2):63-70.
 26. Satapathy, A. K., Gunasekaran, G., Sahoo, S. C., Amit, K., and Rodrigues, P. V. (2009) *Corros Sci* 51:2848.
 27. Akalezi, C.O., Enenebaku, C.K. and Oguzie, E.E. (2012). Application of aqueous extracts of coffee senna for control of mild steel corrosion in acidic environments. *International Journal of Industrial Chemistry*, 3:13-25.
 28. Oguzie, E.E., Adindu, C.B., Enenebeaku, C.K., Ogukwe, C.E., Chidiebere, M.A. and Oguzie, L.L. (2012a). Natural products for materials protection: Mechanism of corrosion inhibition of mild steel by acid extracts of *Piper guineense*. *Journal of Physical Chemistry*, dx.doi.org/10.1021/jp300791s.
 29. Qureshi Absar A. and Eswar Kumar K. (2010). Phytochemical constituents and pharmacological

- activities of *Trachyspermum ammi*, *Plant Archives*, 10: 955-959.
30. Okafor, P. C., Ebenso, E. E., and Ekpe, U. J. (2010). Azadirachta Indica Extracts as Corrosion Inhibitor for Mild Steel in Acid Media. *International Journal of Electrochemical Science*, 5: 978-993.
 31. Eddy, N.O.; Ekwumemgbo, P. and Odoemelam, S.A. (2008). Inhibition of the corrosion of mild steel in H₂SO₄ by 5-amino-1-cyclopropyl-7-[3R,5S] 3,5-dimethylpiperazin-1-yl]-6,8-difluoro-4-oxo quinoline-3-carboxylic acid. *Int. J. Phys. Sci.* 3(11): 1-6.
 32. Lebrini, M., Robert, F., and Roos, C. (2010). Inhibition Effect of Alkaloids Extract from Annona Squamosa Plant on the Corrosion of C38 Steel in Normal Hydrochloric Acid Medium. *International Journal of Electrochemical Science*, 5: 1698-1712.
 33. Singh, A., Singh, V. K., and Quraishi, M. A. (2010). Effect of fruit extracts of some environmentally benign green corrosion inhibitors on corrosion of mild steel in hydrochloric acid solution. *J. Mater. Environ. Sci.*, 162-174.
 34. Loto, C. A. (2011). Inhibition effect of Tea (*Camellia Sinensis*) extract on the corrosion of mild steel in dilute sulphuric acid. *J. Mater. Environ. Sci.*, 2(4): 335-344.
 35. Lebrini, M., Robert, F., and Roos, C. (2011). Alkaloids Extract from *Palicourea guianensis* Plant as Corrosion Inhibitor for C38 Steel in 1M Hydrochloric Acid Medium. *International Journal of Electrochemical Science*, 6: 847-859.
 36. Delley, B. (1990). An All-Electron Numerical Method for Solving the Local Density Functional for Polyatomic Molecules. *Journal of Chemical Physics*, 92:508-517.
 37. Delley, B. (2000). From molecules to solids with the DMol3 approach. *Journal of Chemical Physics*, 113:7756-7764.
 38. Martinez, S. (2003). Inhibitory mechanism of mimosa tannin using molecular modeling and substitutional adsorption isotherms. *Materials Chemistry and Physics*, 77(1):97-102.
 39. Khaled, K.F. (2010b). Corrosion of copper in nitric acid solutions using some amino acids: A combined experimental and theoretical study. *Corrosion Science*, 52:3225-3234.
 40. Rodriguez-Valdez, L. M., Martinez-Villafane, A., Martinez, L., Glossman-Mitnik, D. (2005). Computational simulation of the molecular structure and properties of heterocyclic organic compounds with possible corrosion inhibition properties. *Journal of Molecular Structure (THEOCHEM)*, 713: 65-70.
 41. Fu J, Li S, Cao L, Wang Y, Yan L, Lu L (2010) *J Mater Sci* 45:979. doi:[10.1007/s10853-009-4028-0](https://doi.org/10.1007/s10853-009-4028-0).
 42. Fu J, Li S, Wang Y, Liu X, Lu L (2011) *J Mater Sci* 46:3550. doi: [10.1007/s10853-011-5267-4](https://doi.org/10.1007/s10853-011-5267-4)
 43. Casewit, C.J., Colwell, K.S. and Rappé, A. K. (1992a). Application of a universal force field to organic molecules. *Journal of the American Chemical Society*, 114:10035-10046.
 44. Casewit, C.J., Colwell, K. S. and Rappé, A. K. (1992b). Application of a universal force field to main group compounds. *Journal of the American Chemical Society*, 114:10046-10053.

9/1/2015